Theses and Dissertations   1. Thesis and Dissertation Collection, all items

2022-06

ROBUST ENERGY-AWARE UNMANNED AERIAL VEHICLE ROUTING USING ENSEMBLE WEATHER FORECASTS

Won, David D.

Monterey, CA; Naval Postgraduate School

http://hdl.handle.net/10945/70783

NAVAL POSTGRADUATE SCHOOL

MONTEREY, CALIFORNIA

THESIS

ROBUST ENERGY-AWARE UNMANNED AERIAL
VEHICLE ROUTING USING ENSEMBLE WEATHER
FORECASTS

by

David D. Won

June 2022

Thesis Advisor: Emily M. Craparo
Co-Advisor: Vladimir N. Dobrokhodov
Second Reader: Nicholas Ulmer

Approved for public release. Distribution is unlimited.

THIS PAGE INTENTIONALLY LEFT BLANK

REPORT DOCUMENTATION PAGE		*Form Approved OMB No. 0704-0188*

Public reporting burden for this collection of information is estimated to average 1 hour per response, including the time for reviewing instruction, searching existing data sources, gathering and maintaining the data needed, and completing and reviewing the collection of information. Send comments regarding this burden estimate or any other aspect of this collection of information, including suggestions for reducing this burden, to Washington headquarters Services, Directorate for Information Operations and Reports, 1215 Jefferson Davis Highway, Suite 1204, Arlington, VA 22202-4302, and to the Office of Management and Budget, Paperwork Reduction Project (0704-0188) Washington, DC, 20503.

1. AGENCY USE ONLY *(Leave blank)*	2. REPORT DATE June 2022	3. REPORT TYPE AND DATES COVERED Master's thesis
4. TITLE AND SUBTITLE ROBUST ENERGY-AWARE UNMANNED AERIAL VEHICLE ROUTING USING ENSEMBLE WEATHER FORECASTS		5. FUNDING NUMBERS RMQCA
6. AUTHOR(S) David D. Won		
7. PERFORMING ORGANIZATION NAME(S) AND ADDRESS(ES) Naval Postgraduate School Monterey, CA 93943-5000		8. PERFORMING ORGANIZATION REPORT NUMBER
9. SPONSORING / MONITORING AGENCY NAME(S) AND ADDRESS(ES) ONR, NRL, Arlington, VA 22203		10. SPONSORING / MONITORING AGENCY REPORT NUMBER

11. SUPPLEMENTARY NOTES The views expressed in this thesis are those of the author and do not reflect the official policy or position of the Department of Defense or the U.S. Government.

12a. DISTRIBUTION / AVAILABILITY STATEMENT Approved for public release. Distribution is unlimited.	12b. DISTRIBUTION CODE A

13. ABSTRACT (maximum 200 words)

The Marine Corps seeks to develop energy-aware unmanned aerial vehicle (UAV) routing for last-mile logistics resupply. UAVs have limited range and time on station to execute their assigned mission. To optimize the delivery of supplies to dispersed units, users must optimally utilize the internal energy onboard the UAV while considering external factors such as weather and priorities of resupply requests. Energy-aware UAV routing will increase Marine Corps logistics capabilities during expeditionary advanced base operations (EABO). The current EABO construct places forces within the threat rings of adversary weapon systems. Use of UAVs can allow dispersed forces to operate in the adversary's threat rings without the stoppage of logistical support. This thesis builds upon the two-layer framework developed in previous theses by Jatho (2020) and Haller (2021) to include ensemble weather forecasts and partial delivery of supplies. The first layer, which solves the boundary value problem to obtain optimal trajectories between all nodes in the network, is solved for each member of the ensemble forecast. The second layer consists of a stochastic vehicle routing problem using the cost matrix from the first layer. This thesis also introduces the notion of partial delivery of supplies in the second layer to allow demand nodes to request multiple packages of supplies that can be delivered by multiple UAVs. Finally, this thesis analyzes various case studies and corresponding results.

14. SUBJECT TERMS energy, expeditionary advanced base operations, EABO, unmanned aerial vehicle, UAV, wind, optimize, routing, optimal			15. NUMBER OF PAGES 73
			16. PRICE CODE
17. SECURITY CLASSIFICATION OF REPORT Unclassified	18. SECURITY CLASSIFICATION OF THIS PAGE Unclassified	19. SECURITY CLASSIFICATION OF ABSTRACT Unclassified	20. LIMITATION OF ABSTRACT UU

THIS PAGE INTENTIONALLY LEFT BLANK

ROBUST ENERGY-AWARE UNMANNED AERIAL VEHICLE ROUTING
USING ENSEMBLE WEATHER FORECASTS

David D. Won
Captain, United States Marine Corps
BS, United States Naval Academy, 2016

Submitted in partial fulfillment of the
requirements for the degree of

MASTER OF SCIENCE IN OPERATIONS RESEARCH

from the

**NAVAL POSTGRADUATE SCHOOL
June 2022**

Approved by: Emily M. Craparo
Advisor

Vladimir N. Dobrokhodov
Co-Advisor

Nicholas Ulmer
Second Reader

W. Matthew Carlyle
Chair, Department of Operations Research

iii

THIS PAGE INTENTIONALLY LEFT BLANK

ABSTRACT

The Marine Corps seeks to develop energy-aware unmanned aerial vehicle (UAV) routing for last-mile logistics resupply. UAVs have limited range and time on station to execute their assigned mission. To optimize the delivery of supplies to dispersed units, users must optimally utilize the internal energy onboard the UAV while considering external factors such as weather and priorities of resupply requests. Energy-aware UAV routing will increase Marine Corps logistics capabilities during expeditionary advanced base operations (EABO). The current EABO construct places forces within the threat rings of adversary weapon systems. Use of UAVs can allow dispersed forces to operate in the adversary's threat rings without the stoppage of logistical support. This thesis builds upon the two-layer framework developed in previous theses by Jatho (2020) and Haller (2021) to include ensemble weather forecasts and partial delivery of supplies. The first layer, which solves the boundary value problem to obtain optimal trajectories between all nodes in the network, is solved for each member of the ensemble forecast. The second layer consists of a stochastic vehicle routing problem using the cost matrix from the first layer. This thesis also introduces the notion of partial delivery of supplies in the second layer to allow demand nodes to request multiple packages of supplies that can be delivered by multiple UAVs. Finally, this thesis analyzes various case studies and corresponding results.

THIS PAGE INTENTIONALLY LEFT BLANK

Table of Contents

List of Figures

List of Tables

THIS PAGE INTENTIONALLY LEFT BLANK

List of Acronyms and Abbreviations

BVP   boundary value problem

CMC   Commandant of the Marine Corps

COAMPS   Coupled Ocean/Atmosphere Mesoscale Prediction System

CLB   combat logistics battalion

CLR   combat logistics regiment

CTP   common tactical picture

EAB   expeditionary advanced base

EABO   expeditionary advanced base operations

EVS   expected value solution

GCE   Ground Combat Element

H&S   headquarters and services

ILP   integer linear programming

MDMTSP   multiple depot multiple traveling salesman problem

MDVRP   multiple depot vehicle routing problem

MILP   mixed-integer linear problem

MLG   Marine Logistics Group

mTSP   multiple traveling salesperson problem

PIS   perfect information solutions

PMP   Pontryagin's maximum principle

TSP   traveling salesperson problem

UAV   unmanned aerial vehicle

ULS-A   Unmanned Logistics Systems - Air

USMC   United States Marine Corps

VRP   vehicle routing problem

WEZ   weapons engagement zone

Wh   watt-hours

Executive Summary

Conflicts against near-peer adversaries have changed the way the United States Marine Corps (USMC) seeks to employ its operating forces. Future conflicts will consist of technologically saturated battlefields leading to the employment of stand-in forces that conduct distributed operations away from main lines of communications and logistical support. To support a dynamic battlefield that will be restrictive in the areas of signature management and freedom of movement, the USMC seeks to employ low-risk but high-payoff UAVs to conduct last-mile resupply missions. Work conducted in this thesis supports this effort by creating a UAV routing tool for Marine Corps logisticians.

This thesis implements a two-layer approach and includes ensemble weather forecasts. Ensemble weather forecasts are a family of weather forecasts that capture the uncertainty inherent in weather prediction. The first layer solves for the optimal costs to fly between each pair of nodes in the supply network, while the second layer utilizes MDVRP to find the UAV routes that maximize the fulfillment of prioritized requests at demand nodes while minimizing the worst and average case energy consumption across all ensemble members. This thesis modifies both layers to utilize ensemble weather forecasts. In the first layer, costs are calculated for each ensemble member. Then, in the second layer, the MDVRP ensures that the selected routes are energy feasible for all UAVs for every ensemble member. The UAV routing provided by the ensemble weather model is more conservative than the UAV routing for deterministic weather models. However, the ensemble weather model provides UAV routes that have a greater probability of mission success.

The second contribution of this thesis enables partial delivery of supplies where demand nodes have the ability to request multiple discrete packages of supplies. The implementation of partial deliveries allows UAVs to work collectively to fulfill demands in the network, providing the logistician greater flexibility in mission planning.

The final portion of this thesis explores a scenario involving an infantry battalion conducting distributed operations across multiple islands while supported by a combat logistics battalion (CLB) and combat logistics regiment (CLR). A second scenario is also conducted to explore methods to increase organic support prior to requesting logistics support from

higher headquarters.

Acknowledgments

Thank you to my advisors Professor Emily Craparo and Professor Vladimir Dobrokhodov for the guidance, patience and support during the development of this thesis.

I would like to thank my family for their continued support during my time in the USMC and at NPS.

THIS PAGE INTENTIONALLY LEFT BLANK

CHAPTER 1:
Introduction

> The proliferation of long-range precision fires in the future battlespace will significantly impact logistics as well as operations. WWI metaphors of an extended 'no man's land' are worthy descriptions of what should be anticipated. Forces that remain within the enemy long-range weapons engagement zone will have to actively plan passive defenses to remain effective, and will be dependent upon logistics service support and supply systems that are equally active and resilient. A fully integrated, active maritime defense-in-depth will be able to inflict disproportionate result on adversary forces, but that defense will consume vast quantities of ordnance in intense battles of indeterminate duration. In effect, a race will take place between a willful adversary attempting to mass forces at the point he chooses as decisive, and the ability of defensive forces to supply munitions, relieve forces, and support services to the defenders. (United States Marine Corps 2018, p. 61)

The shift in focus from conflicts in the Middle East to fighting our adversaries in the Pacific presents a unique set of challenges for United States Marine Corps (USMC) planners. Contrary to most recent conflicts in the Middle East, our adversaries now possess the same if not greater technological capabilities. This creates a battlefield saturated with equipment capable of electronic warfare, sensing, long-range fires and naval battles.

To combat the adversary's capabilities, the Commandant of the Marine Corps (CMC) seeks to employ stand-in forces that operate within the weapons engagement zone (WEZ) of enemy weapon systems. According to the CMC, "stand-in forces are designed to generate technically disruptive, tactical stand-in engagements that confront aggressor naval forces with an array of low signature, affordable, and risk-worthy platforms and payloads" (Berger 2019, p. 10). Stand-in forces will often be far from the lines of communication and operate in dispersed locations throughout the battlefield. The dispersed nature of stand-in forces seeks to create friction for the adversary and closely resembles saturation tactics where the adversary's domains are overwhelmed and slow to respond.

The construct of stand-in forces to combat near peer adversaries calls for a new strategy of lo-

gistical support. To meet the support requirements, the CMC has emphasized expeditionary advance base operations (EABO). A new concept to the USMC, "The EABO concept creates the ability and requirements to position flotillas, UXX squadrons, land-based anti-ship missiles, logistics support, and other innovative Navy capabilities forward to enable persistent naval presence and influence" (USMC 2018, p. 22). Expeditionary advance bases (EABs) will provide logisticians an area to conduct last mile logistics to sustain the stand-in forces.

Support from EABs will be vastly different compared to traditional support concepts that employ large signature methods such as large bases, convoys, stockpiles of supplies, and numerous support personnel. Support concepts will include autonomous vehicles that are low in signature, cost, and risk. While the operational USMC forces currently do not have these assets, senior leaders have acknowledged that "EABO will require a new concept of logistical support and sustainment, and demand innovative platforms to execute novel distribution and delivery requirements" (USMC 2018, p. 48). The EABO handbook published in 2018 provides insight into the technology surrounding the future of USMC logistics:

> Once specific EABO logistics requirements are determined, the innovation base of America's military research and development (RD) facilities and leading industries are ready to deliver creative solutions that take advantage of the fast advancing technical revolution in power generation and storage, additive manufacturing, autonomy, AI, electric engines, energy harvesting, and a host of other new technical and scientific endeavors that can be focused on innovation in the field of military logistics. (USMC 2018, p. 65)

Unmanned aerial vehicles (UAVs), commonly known as drones, provide an option for logistics planners in EABO. UAVs are low-signature and present less risk than manned platforms in a contested environment. The employment of UAVs at the battalion level requires planning tools that allow logistic planners to determine the most optimal flight path and depot selection for a given situation. The current logistics cells do not have these planning assets.

1.1   Research Objective and Methodology

The objective of this thesis is to integrate ensemble weather forecasts into a UAV routing model for planning logistics operations. This thesis builds upon the two-stage framework developed by Jatho (2020) and Haller (2021). The first-stage, which solves the boundary value problem (BVP) to obtain optimal trajectories between all nodes in the network, is instead solved for each member of the ensemble forecast. This results in a family of cost matrices, one for each ensemble member. This family of cost matrices then serves as input to the second-stage multiple depot vehicle routing problem (MDVRP) model, which determines the optimal UAV routing. Employing an ensemble forecast model to this problem results in a more robust optimization approach.

This thesis also explores partial delivery of packaged supplies to demand nodes. We establish requests from operating units as discrete packages and allow units to request multiple packages of various items at different priority levels. This allows greater flexibility for both the stand-in forces and logistics planners for resupply missions. Figure 1.1 highlights the previous work conducted by Jatho (2020) and Haller (2021) and the work conducted in this thesis.
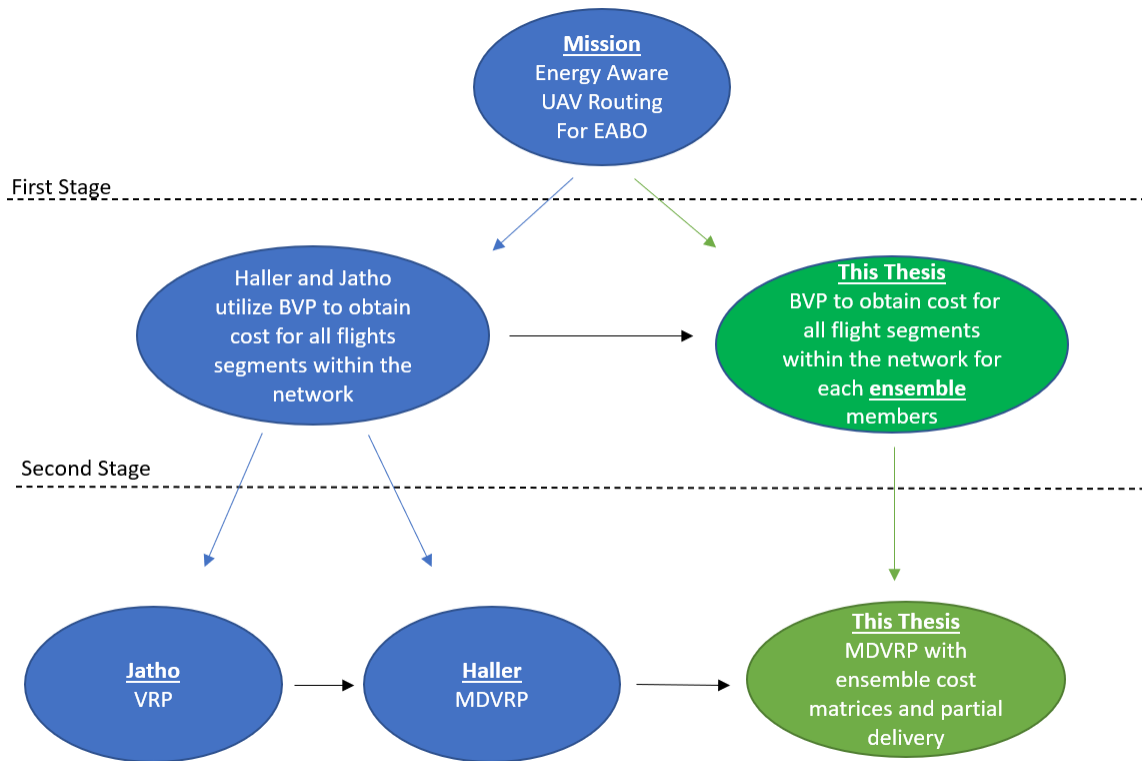
Figure 1.1. Previous work conducted by Jatho (2020) and Haller (2021) is indicated in blue. Jatho and Haller implement the vehicle routing problem (VRP) and the MDVRP, respectively, in the second stage. Work conducted in this thesis is indicated in green. The first part of this thesis solves for costs for all ensemble members and implement the MDVRP in the second stage. This thesis also explores partial delivery of requests at demand nodes.

CHAPTER 2:
Background

Previous work by Jatho (2020) establishes a two-stage optimization problem where the first stage provides energy-optimal flight paths and associated costs between all nodes within the area of operations, given surrounding weather conditions. Jatho then implements a VRP in the second stage to maximize the priority of the demand nodes serviced by the UAV. Haller (2021) expands on work conducted by Jatho to allow UAVs to operate from multiple depots by implementing the MDVRP, which is derived from the multiple depot multiple traveling salesman problem (MDMTSP).

2.1   Review of First Stage

While great circle paths are the shortest path for UAV flight between two locations, they may not be the most energy- or time-efficient routes. Based on work conducted by Dobrokhodov et al. (2020), Jatho's first stage layer derives the energy-optimal route by implementing the BVP, which is solved by applying the Pontryagin's maximum principle (PMP).

Jatho (2020) defines an optimization problem of finding the optimal controls of the UAV while minimizing energy expenditure. The UAV is forbidden from entering no fly zones, and controls are defined as inputs that determine the heading and airspeed for a given UAV's flight trajectory. The cost incurred by UAVs during a flight explicitly accounts for the time-varying wind along the flight segment that is provided by Coupled Ocean/Atmosphere Mesoscale Prediction System (COAMPS) wind profiles. We assume the start time of the mission to be given and the costs are calculated based on the same start time. When the cost is obtained for every segment of the network, the resulting cost matrix provides deterministic wind costs through the duration of each flight segment within the network.

The first stage results in an asymmetric cost matrix for all pairs of nodes i and j, and a plot of the routes between all flight segments. Figure 2.1, shows great circle routes in blue and energy-optimal routes in red. Some great circle and energy-optimal routes overlap. However, many energy-optimal routes vary significantly from the great circle route. Due to these variances, it is important that UAVs with limited energy resources take the energy-optimal

route. Thus, computations in the second stage utilize the cost matrix from energy-optimal flight segments.
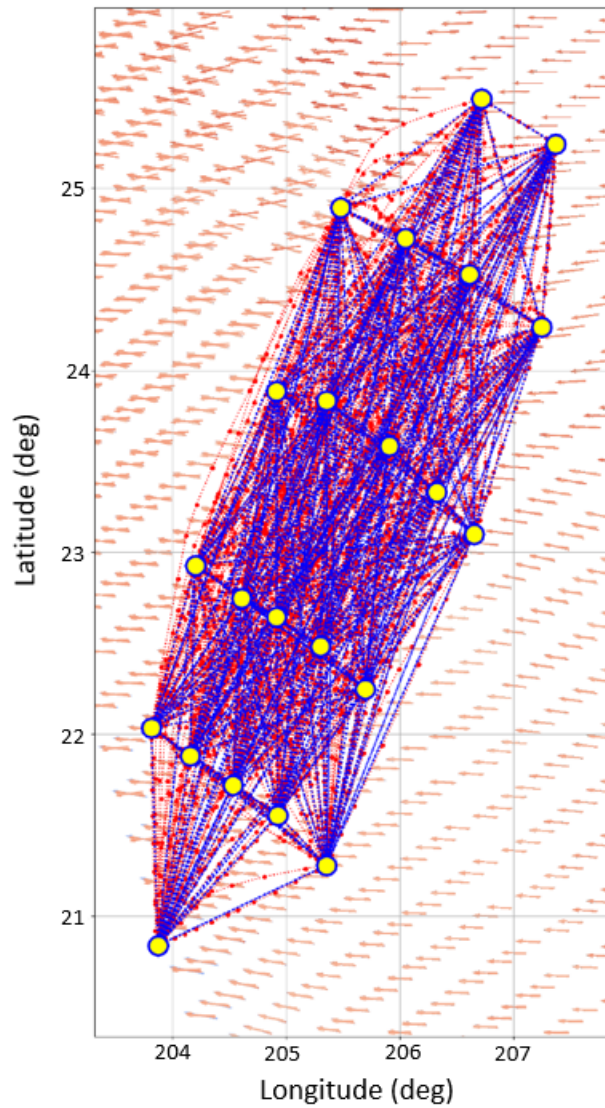
Figure 2.1. Red routes are energy-optimal routes while blue routes are great circle routes. Source: Jatho (2020) Figure 5.8.

Dobrokhodov et al. (2020) dives deeper into an individual flight segment to present the different characteristics of each route. Figure 2.2 displays the wind profile along the UAV flight path, where the blue gradients are head winds and red gradients are tail winds. The

energy-optimal route seeks a path that limits the exposure to headwinds while harnessing the benefits of tailwinds.
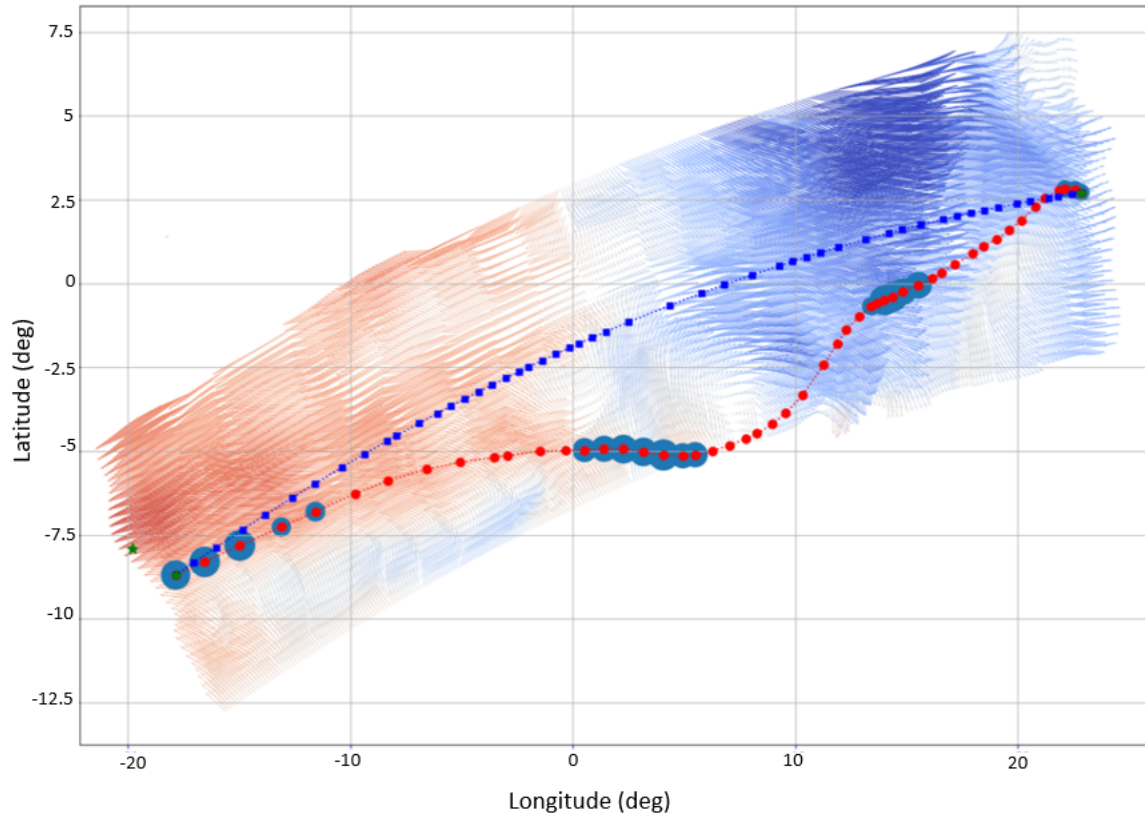
Figure 2.2. Energy-optimal route shown in red and great circle route shown in blue. Source: Dobrokhodov et al. (2020) Figure 11a.

Visually, the energy optimal route is much longer than the great circle route. However, Figure 2.3 shows that the energy-optimal route has significantly higher ground speeds and a shorter flight time compared to the great circle route. The dotted blue line in Figure 2.3 shows the heading of the energy-optimal route, while the ground speeds of the energy-optimal and great circle routes are shown by solid red lines and dotted red lines, respectively.
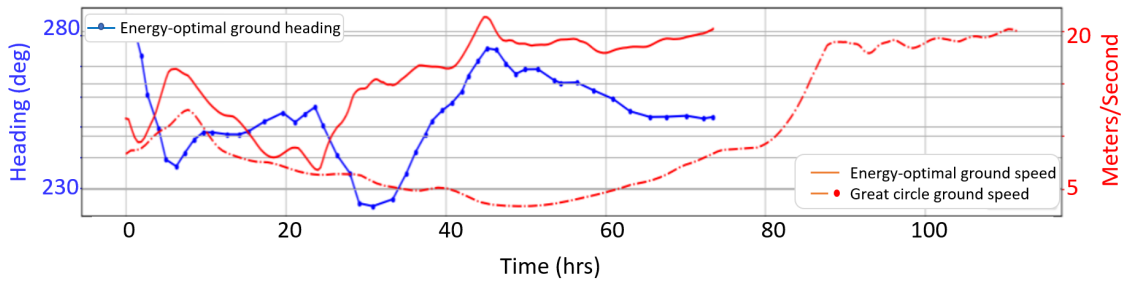
Figure 2.3. Ground speed and overall flight time between energy-optimal route and great circle route. Source: Dobrokhodov et al. (2020) Figure 11b.

2.2 Review of Jatho's Second Stage

The asymmetric cost matrix from the first stage serves as input data into the second stage, which solves the UAV routing problem. Jatho (2020) optimizes the UAV routing by implementing the VRP. The VRP is derived from the traveling salesperson problem (TSP) and multiple traveling salesperson problem (mTSP).

Traveling salesman Problem and Multiple Traveling salesman Problem

The TSP utilizes a mixed-integer linear problem (MILP) to obtain the optimal routing of a salesman within a network of nodes and arcs. The TSP seeks to minimize the cost for one salesman to travel from an initial node and visit all other nodes within the network. Each arc (i, j) within the network has an associated cost c_{ij}, and x_{ij} is a binary variable that takes the value 1 if arc (i, j) is used by the salesman and 0 otherwise. Jatho (2020) builds upon the TSP formulation from Miller et al. (1960).

The mTSP builds on TSP by introducing multiple salesmen to the network. The constraints of the mTSP limit multiple salesmen from visiting the same node while the objective function seeks to minimizing the total cost of travel. Formulation of the mTSP implements an additional index k to represent the multiple salesmen. Binary variable, x_{ijk} takes the value of 1 if salesman k travels along arc ij and 0 otherwise. Jatho (2020) builds upon the mTSP formulation from Kaempfer and Wolf (2019).

Vehicle Routing Problem

The VRP is an extension of the mTSP and is tailored towards routing vehicles, instead of a salesman, through a network. Work conducted by Cheng et al. (2018) discusses a formulation that minimizes the UAV travel distance while subject to constraints such as UAV energy consumption, UAV payload capacity, and scheduling to meet desired time windows.

Dorling et al. (2018) propose two formulations for a multi-trip VRP. The first method minimizes costs while constrained to delivery time limits. The second method minimizes delivery time while constrained to fixed budgets. Jatho (2020) considers a single trip for each UAV and allows some nodes to go unvisited if UAV energy constraints do not allow all nodes to be visited.

Jatho also discusses the dynamic VRP developed by Jaillet and Lu (2011), including both offline and online variants. An offline problem has a predetermined set of nodes for the UAV to visit, while an online problem dynamically adds and drops nodes to a mission. Jatho (2020)'s formulation is offline in nature, i.e., requirements do not change mid-flight.

2.3   Review of Haller's Second Stage

Multiple Depot Multiple Traveling Salesman Problem

The foundation of Haller's formulations Haller (2021) is the MDMTSP, which is an extension of the mTSP. MDMTSP provides flexibility for mission planning by allowing UAVs to operate from multiple depots.

Haller (2021) discusses various publications describing different formulations, and he cites work conducted by Kara and Bektas (2006) as being the closest to his formulation. Kara and Bektas (2006) utilize integer linear programming (ILP) to implement two types of MDMTSP problems which they call fixed and nonfixed destination problems. Both problems require the salesman to visit each customer exactly once, but each salesman is constrained to return to his original depot in the fixed destination problem. The nonfixed destination problem provides additional flexibility by removing the constraint that forces the salesman to return to the starting depot but requires each depot to have the same number of salesman at the end as it was in the beginning. Haller approaches his formulation similar to the nonfixed destination

problem but removes the constraint that requires salesmen to service all customers.

Multiple Depot Vehicle Routing Problem

The MDVRP is related to the MDMTSP but contains constraints related to the vehicle energy consumption and payload capacity. Haller (2021) uses work from Samsuddin et al. (2018) to explain the challenges of identifying optimal depots that can service nodes within the constraints of the UAV energy capacity. Due to the complex nature of the problem, Samsuddin et al. (2018) solve the problem through metaheuristic methods. Haller (2021) implements an exact algorithm to solve MDVRP as he assumes there will be less than 50 demand nodes during EABO.

2.3.1 Ensemble Weather Models

Leutbecher and Palmer (2007) discuss how perturbations to the initial conditions from which forecasts are predicted from lead to weather forecasting errors. An ensemble weather model seeks to mitigate this uncertainty by establishing a finite set of equally probable weather forecasts. Each weather forecast within an ensemble starts on different points of the initial weather probability distribution and is integrated forward in time to obtain weather predictions. Due to variances in starting conditions, each weather prediction within an ensemble will have a different end state at the conclusion of the integration. While differing initial conditions have less of an influence in near future weather predictions, predictions over longer lead times are heavily influenced by the different initial conditions. Figure 2.4 by Craparo et al. (2017) provides a plot that displays the greater variations in wind speed predictions at longer lead times.
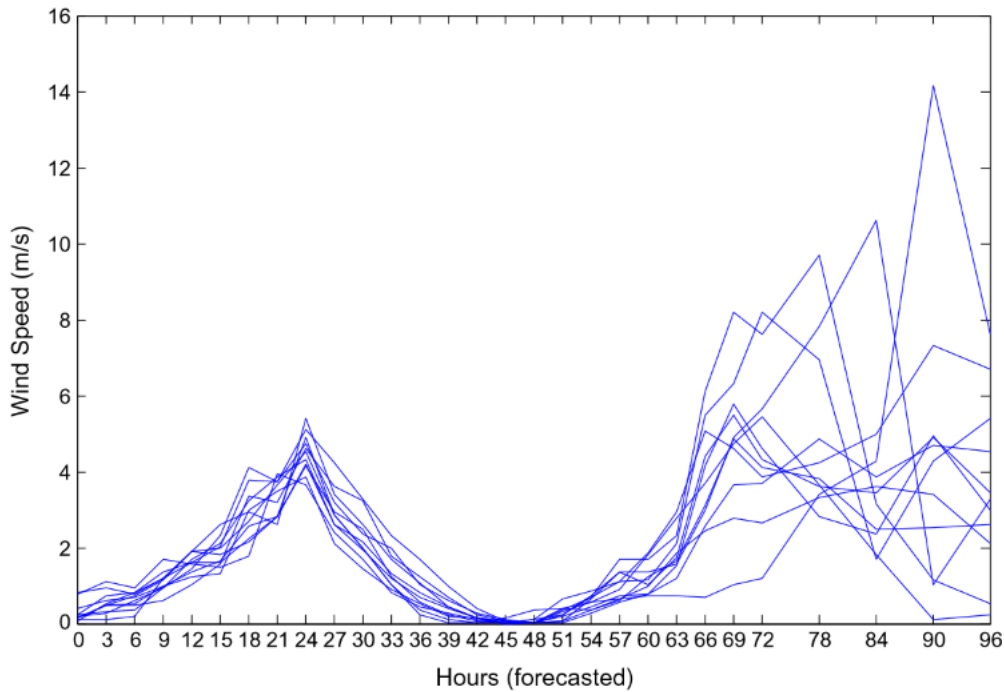
Figure 2.4. Plot shows longer lead time resulting in greater variation in wind speed predictions. Source: Craparo et al. (2017) Figure 1.

Work conducted by Craparo et al. (2017) focuses on utilizing ensemble weather models to optimize microgrid operations for renewable energy sources. The goal of the optimization problem is to minimize cost of operations while constrained to operating characteristics of equipment at the microgrids. To present the robustness of ensemble weather models, Craparo et al. (2017) compares the microgrid performance by optimizing over all 11 ensemble wind forecasts (optimized over all), a single wind forecast that is the average of the ensemble members (optimized for expected wind), a single renewable power production that is the average of the renewable power production of all 11 ensemble members (optimized for expected renewable power), and by selecting a single scenario from the 11 ensemble members (single scenario). The measure of performance for the optimization model is the difference in cost to an omniscient solution where the model has accurate wind predictions. Results in Figure 2.5 show the ensemble weather model having the greatest probability of achieving a cost similar to the omniscient solution.
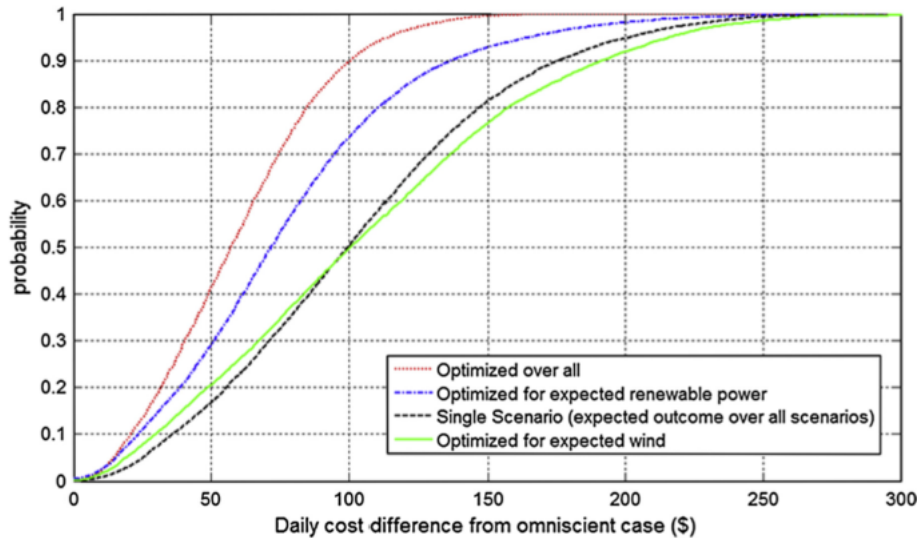
Figure 2.5. When an ensemble weather forecast is available, an optimization model that utilizes this forecast has the greatest probability of achieving a cost similar to the omniscient solution. Source: Craparo et al. (2017) Figure 3.

The work of Franco et al. (2017) concerning airplane routing using ensemble weather models closely resembles the work done in this thesis. This study illustrates fuel consumption of an airplane by through a four-member ensemble model for a cross Atlantic flight between Leonardo da Vinci International Airport and John Fitzgerald Kennedy International Airport. The first method is labeled the expected value solution (EVS) where one flight trajectory is determined by averaging the wind fields across all ensemble members. The second method, called the perfect information solutions (PIS), determines flight trajectories for each ensemble member and averages the fuel consumption across all trajectories. In this particular scenario, the study found the fuel consumption for the EVS to be consistently lower compared to the fuel consumption of the PIS. Franco et al. (2017) conclude the EVS and PIS can be established as upper and lower bounds respectively for airplane fuel consumption. In contrast to work by Franco et al. (2017), this thesis incorporates both the worst case energy consumption and the average energy consumption across all ensemble members into the objective function.

Ensemble Weather Model for EABO

A visual representation of a 10-member ensemble weather model can be seen in Figure 2.6. The network consists of ten-nodes, with great circle routes shown in blue and energy-efficient routes shown in red. Since the ensemble model is comprised of ten-members, ten different energy-efficient routes are shown for each flight segment in the network. The general wind direction is represented by the blue arrows that point from west to east.
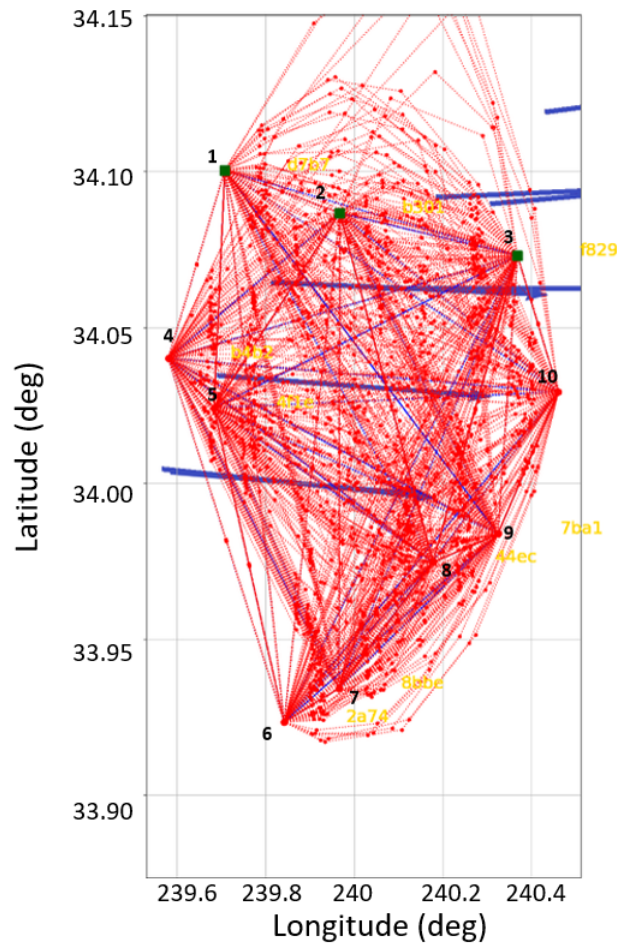
Figure 2.6. Ten-node network with a ten-member ensemble weather model. Each flight segment has ten different energy-efficient routes.

Plots in Figure 2.7 contain ensemble cost distributions for all flight segments in a ten-node network. For each pair of nodes i and j, where $i < j$, the top plot contains the cost distribution of flight segments from node i to node j while the bottom plot contains the

distribution of returning flights from node j to node i.
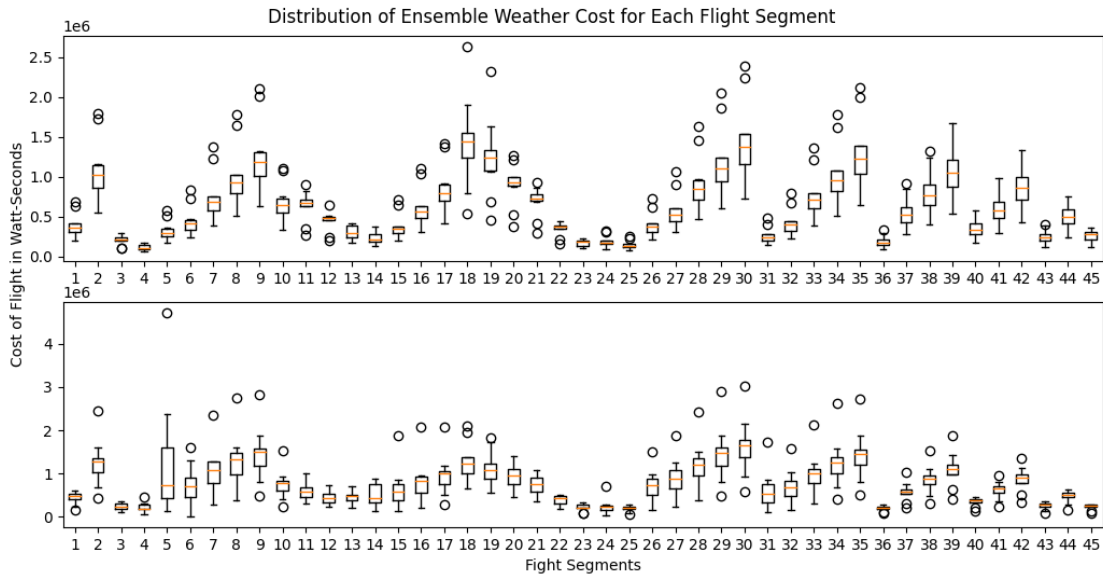
Figure 2.7. Distribution of cost within each ensemble member for all flight segments. Top plot depicts flights from node i to node j. Bottom plot depicts flights from node j to node i.

To aid in understanding of the flight segments, Table 2.1 displays the corresponding nodes i and j for each flight segment in the top plot of Figure 2.7. For example, flight segment one in the top plot depicts the wind variance for UAV flight between nodes one and two. Flight segments for the bottom plot in Figure 2.1 are simply in the reverse direction.

Table 2.1. Flight segments for top plot in Figure 2.7

Flight Segment	Node (i)	Node (j)	Flight Segment	Node (i)	Node (j)	Flight Segment	Node (i)	Node (j)
1	1	2	16	2	9	31	5	6
2	1	3	17	2	10	32	5	7
3	1	4	18	3	4	33	5	8
4	1	5	19	3	5	34	5	9
5	1	6	20	3	6	35	5	10
6	1	7	21	3	7	36	6	7
7	1	8	22	3	8	37	6	8
8	1	9	23	3	9	38	6	9
9	1	10	24	3	10	39	6	10
10	2	3	25	4	5	40	7	8
11	2	4	26	4	6	41	7	9
12	2	5	27	4	7	42	7	10
13	2	6	28	4	8	43	8	9
14	2	7	29	4	9	44	8	10
15	2	8	30	4	10	45	9	10

A general observation is that flight segments that experience cross winds seem to have less variance in cost over all ensemble members. Flights that experience head or tail wind have greater variance in cost and within those flights, longer distance flights seems to have the greatest variance in cost across all ensemble members.

THIS PAGE INTENTIONALLY LEFT BLANK

CHAPTER 3:
Energy-Optimal Routing with Ensemble Weather Forecasts

3.1 Introduction

The ensemble weather model formulation expands on previous formulations conducted by Jatho (2020) and Haller (2021). Their models allow UAVs to utilize multiple depots to maximize the rewards at serviced nodes while decreasing overall energy expenditure.

The first stage of this model, which produces the cost matrix, now provides multiple cost matrices, one for each of a predetermined number of ensemble members. This model provides a more robust formulation by accounting for uncertainty in the weather forecast, leading to a higher likelihood of successful UAV flights.

3.2 Assumptions

Several assumptions are made regarding the characteristics of the UAV and the classification of the supplies. In the first layer, the energy costs produced by the BVP are obtained by using a nominal UAV. Costs between flight segments are based on a full UAV payload at takeoff and during the entire flight. Therefore, the resulting cost matrix provides a conservative estimate; UAVs will not necessarily be fully loaded at takeoff and will lighten their loads as the make deliveries along their routes. As for the supplies, we assume requests from demand nodes are discrete (i.e., not divisible among multiple UAVs) and that the only relevant information regarding a demand is the weight of the required item. This implies that UAVs do not have space restrictions, all UAVs may carry all types of item requested, and all supply depots are infinitely stocked with all items that may be requested.

3.3 Indices and Sets

Set N is indexed by i, j and r and represents all nodes within the network. Sets P and Q are subsets of set N and represent depot nodes and demand nodes, respectively. Weather

17

forecast ensemble members are represented by set E, indexed by e. Set M, indexed by k, represents UAVs.

3.4   Data

Data is sourced into the model by user inputs and from the solution of the BVP in the first stage. USMC planners must input demands at each node j with associated weights (d_j) in pounds. Further inputs include the carrying capacity s_k of the each UAV (in pounds), starting node for each UAV (b_k), energy capacity of each UAV $(EnergyMax_k)$ in watt-hours (Wh) and demand importance at each demand node j to determine the reward (R_j) obtained by the UAVs. Demands are labeled as routine, priority and urgent. The reward for servicing a priority-level demand is five time greater than servicing a routine-level demand, and the reward for servicing an urgent-level demand is 10 times greater than servicing a routine-level demand.

The solution from the first stage provides costs incurred by the UAVs in watt-hours for each flight segment within the network. Data for cost is annotated by C_{ijke}, which represents the energy cost for UAV k to fly from node i to node j in ensemble member e.

3.5   Decision Variables

Three decision variables for this model are X_{ijk}, u_i and Z. X_{ijk} is a binary variable that takes the value 1 if UAV k flies in the flight segment between node i and j.

$$X_{ijk} = \begin{cases} 1, & \text{if UAV } k \text{ travels from node } i \text{ to node } j \\ 0, & \text{otherwise} \end{cases} \quad (3.1)$$

Variable u_i restricts the UAVs from making subtours. A subtour occurs when a UAVs flies among a subset nodes in a cycle, but the cycle is not connected to a depot node or to the remainder of the UAV's path.

$$u_i \in \mathbb{Z} \qquad\qquad \forall i \in Q \qquad\qquad (3.2)$$

Variable Z calculates the maximum energy consumed by any UAV across all ensemble members.

$$Z > 0 \tag{3.3}$$

3.6 Objective Function

The objective function, shown below, has three different features.

$$\max \sum_{i=1}^{n} \sum_{j:j\neq i} \sum_{k=1}^{m} X_{ijk} R_j - \gamma Z - \epsilon \sum_{i=1}^{n} \sum_{j:j\neq i} \sum_{k=1}^{m} \sum_{e=1}^{E} X_{ijk} \frac{C_{ijke}}{|E|} \tag{3.4}$$

The first term of the objective function ($\max \sum_{i=1}^{n} \sum_{j:j\neq i} \sum_{k=1}^{m} X_{ijk} R_j$) maximizes the reward ($R_j$) obtained by the UAVs for servicing demand nodes j. This is the primary objective of the model; the remaining two terms act as tie-breakers. The second term of the objective function (γZ) seeks to minimize the maximum energy expended by any UAV across all ensemble members. The γ variable is an user-input penalty for the most energy-expensive route. The third term in the objective function ($\epsilon \sum_{i=1}^{n} \sum_{j:j\neq i} \sum_{k=1}^{m} \sum_{e=1}^{E} X_{ijk} \frac{C_{ijke}}{|E|}$) accounts for the average energy cost across all ensemble members. This term determines the flight path for all other UAVs besides the single UAV that has the largest energy expenditure. Within a set of energy-feasible routes that visit the optimal set of demand nodes, this term rewards the most energy-efficient route. The ϵ variable is another user-determined penalty.

3.7 Constraints

The constraints are an evolutionary expansion from the mTSP and MDVRP to reflect the impacts of the ensemble weather model.

3.7.1 Constraints from mTSP

Constraints below are derived from the mTSP and ensure UAV flight segments are planned in accordance with the baseline mTSP model.

$$\sum_{j \in Q} X_{b_k j k} \leq 1 \qquad \forall \, k \in \{1, ...m\} \qquad (3.5)$$

$$\sum_{i \in Q} \sum_{j \in P} X_{ijk} \leq 1 \qquad \forall \, k \in \{1, ...m\} \qquad (3.6)$$

$$\sum_{i=1}^{n} \sum_{k=1}^{m} X_{ijk} \leq 1 \qquad \forall \, j \in Q \qquad (3.7)$$

$$\sum_{j=1}^{n} \sum_{k=1}^{m} X_{ijk} \leq 1 \qquad \forall \, i \in Q \qquad (3.8)$$

$$\sum_{i \in N} X_{irk} = \sum_{j \in N} X_{rjk} \qquad \forall \, r \in Q; k \in \{1, ...m\} \qquad (3.9)$$

$$u_i - u_j + (n - m) * \sum_{k=1}^{m} X_{ijk} \leq n - m - 1 \qquad \forall \, i, j \in Q \qquad (3.10)$$

Constraint 3.5 forces each UAV, if chosen to leave its depot, to depart its starting depot b_k exactly once. Constraint 3.6 allows each UAV to return to any depot within the network. However, each UAV may return to a depot at most once during its route.

Constraints 3.7, 3.8 and 3.9 accomplish similar effects on the UAV routes. Constraints 3.7 and 3.8 ensure there is at most one entry and one exit per demand node by all UAVs in the network. Constraint 3.9 serves as a flow conservation constraint and ensures the number of entries and exits at demands nodes are equal to each other. Secondary effect of these constraints is that multiple UAVs will not visit the same demand nodes.

Constraint 3.10 ensures degenerate subtours are eliminated from the UAV routes. This constraint is from Miller et al. (1960).

3.7.2 Constraints for Multiple Depots

$$\sum_{j \in Q} X_{b_k j k} = \sum_{i \in Q} \sum_{j \in P} X_{ijk} \qquad \forall\, k \in \{1, ... m\} \qquad (3.11)$$

In constraint 3.11, a UAV that leaves a depot node must return to a depot to finish its route. However, this constraint does not force an UAV to finish its flight segments at its initial starting depot node.

3.7.3 Constraints for UAV Performance and Ensemble Weather Model

Expanding on the mTSP, the constraints below are UAV- and weather-specific constraints derived from the MDVRP model.

$$\sum_{i=1}^{n} \sum_{j:j \neq i} d_j X_{ijk} \leq s_k \qquad \forall\, k \in \{1, ... m\} \qquad (3.12)$$

$$\sum_{i=1}^{n} \sum_{j:j \neq i} C_{ijke} X_{ijk} \leq EnergyMax_k \qquad \forall\, e \in E; \forall\, k \in \{1, ... m\} \qquad (3.13)$$

Constraint 3.12 ensures the total demand serviced by each UAV does not exceed the payload capacity (s_k) of the UAV. Constraint 3.13 ensures the route for each UAV is energy feasible for all ensemble members.

$$Z \geq \sum_{i=1}^{n} \sum_{j:j \neq i} \sum_{k=1}^{m} C_{ijke} X_{ijk} \qquad \forall\, e \in E \qquad (3.14)$$

In constraint 3.14, variable Z takes on the value of the worst-case energy expenditure of a single UAV across all ensemble members. This allows variable Z to be incorporated into the objective function to account for the worst case energy scenario.

3.8 Complete Formulation

Our complete formulation appears below. Additions to the models of Jatho (2020) and Haller (2021) are indicated in red.

Sets and Indices:

$i, j \in N = \{1, ..., n\}$ Nodes

$k \in M = \{1, ..., m\}$ UAVs

$e \in E = \{1, ..., e\}$ Ensemble members

$P \subseteq N$ Depot nodes

$Q \subseteq N$ Demand nodes

Data:

C_{ijke} = Energy for UAV k to travel from node i and node j for ensemble member e [Wh]

d_j = Demand at node j [Pounds]

s_k = Capacity of UAV k [Pounds]

b_k = Starting depot of UAV k

$EnergyMax_k$ = Energy capacity of UAV k [Wh]

ϵ = Penalty weight

γ = Penalty weight

R_j = Reward for delivering supplies to node j, based on demand priority

Decision Variables:

X_{ijk} = Binary variable representing whether or not UAV k travels from node i to node j

Z = Maximum energy consumption by any UAV

u_i = Dummy variable to prevent degenerate subtours

$$\max \sum_{i=1}^{n} \sum_{j:j\neq i} \sum_{k=1}^{m} X_{ijk} R_j - \gamma Z - \epsilon \sum_{i=1}^{n} \sum_{j:j\neq i} \sum_{k=1}^{m} \sum_{e=1}^{E} X_{ijk} \frac{C_{ijke}}{|E|} \qquad (3.15)$$

$$Z \geq \sum_{i=1}^{n} \sum_{j:j\neq i} \sum_{k=1}^{m} C_{ijke} X_{ijk} \qquad \forall\, e \in E \qquad (3.16)$$

$$\sum_{j\in Q} X_{b_k jk} \leq 1 \qquad \forall\, k \in \{1,...m\} \qquad (3.17)$$

$$\sum_{i\in Q} \sum_{j\in P} X_{ijk} \leq 1 \qquad \forall\, k \in \{1,...m\} \qquad (3.18)$$

$$\sum_{i=1}^{n} \sum_{k=1}^{m} X_{ijk} \leq 1 \qquad \forall\, j \in Q \qquad (3.19)$$

$$\sum_{j=1}^{n} \sum_{k=1}^{m} X_{ijk} \leq 1 \qquad \forall\, i \in Q \qquad (3.20)$$

$$\sum_{i\in N} X_{irk} = \sum_{j\in N} X_{rjk} \qquad \forall\, r \in Q; k \in \{1,...m\} \qquad (3.21)$$

$$\sum_{j\in Q} X_{b_k jk} = \sum_{i\in Q} \sum_{j\in P} X_{ijk} \qquad \forall\, k \in \{1,...m\} \qquad (3.22)$$

$$u_i - u_j + (n-m) * \sum_{k=1}^{m} X_{ijk} \leq n - m - 1 \qquad \forall\, i,j \in Q \qquad (3.23)$$

$$\sum_{i=1}^{n} \sum_{j:j\neq i} d_j X_{ijk} \leq s_k \qquad \forall\, k \in \{1,...m\} \qquad (3.24)$$

$$\sum_{i=1}^{n} \sum_{j:j\neq i} C_{ijke} X_{ijk} \leq EnergyMax_k \qquad \forall\, e \in E; \forall\, k \in \{1,...m\} \qquad (3.25)$$

$$X_{ijk} \in \{0,1\} \qquad \forall i,j \in \{1,...n\} \qquad (3.26)$$

$$u_i \in \mathbb{W} \qquad \forall i \in Q \qquad (3.27)$$

$$Z > 0 \qquad (3.28)$$

3.9   Model Output

We implement the model in Python using the Pyomo software package (version 6.1.2) and solve it using the CPLEX solver (version 22.1.0.0) on a machine with 1.60 GHz Intel Core i5 CPU with 8 GB of RAM. The output of the model includes the value of the objective function, energy expended by each UAV and a graph that includes all depots and nodes with UAV flight paths. To demonstrate a model output, we employ the network and wind profile

in Figure 2.6 with the characteristics outlined in Table 3.1.

Table 3.1. Data for demand nodes and UAVs.

Demand Node	Demand Type & Amount
4	15 Urgent
5	15 Urgent
6	15 Urgent
7	15 Urgent
8	15 Urgent
9	15 Urgent

UAV	Payload Capacity (lbs)	Energy (Wh)	Starting Depot
1	30	1,000,000	1
2	30	1,000,000	2
3	30	1,000,000	3

This scenario contains 130 constraints, 278 variables and yields an optimal solution in 0.213 seconds. The objective function value is 189,044,37,027 with 60 units of supplies provided across all demand nodes. UAV one's flight path is $1 \rightarrow 5 \rightarrow 4 \rightarrow 1$ and expends 701,467 Wh of energy. UAV three's flight path is $3 \rightarrow 10 \rightarrow 9 \rightarrow 3$ and expends 761,393 Wh of energy. The model does not employ UAV two in this scenario. The flight path of the UAVs can be seen in Figure 3.1.
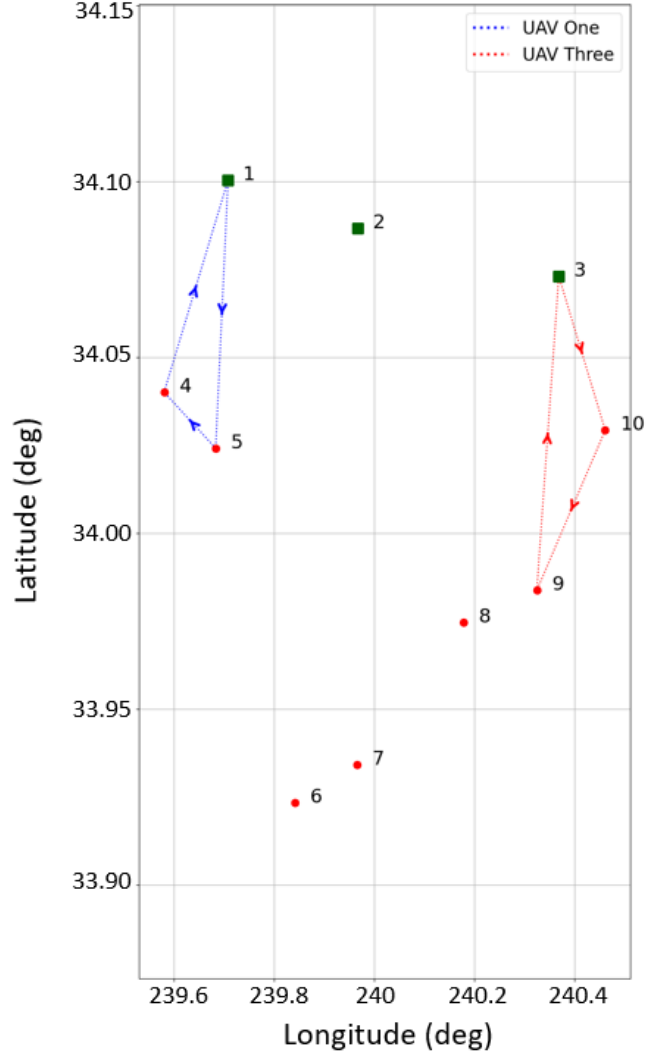
Figure 3.1. Flight path for UAV one and UAV two.

To gain an insight into UAV two's inactivity, we modify constraint 3.17 as follows:

$$\sum_{j \in Q} X_{b_k jk} \geq 1 \qquad\qquad \forall\, k \in \{1, ... m\} \qquad\qquad (3.29)$$

Constraint 3.29 ensures all UAVs depart their starting depot nodes, which is a deviation from the original formulation where the model has the ability to keep UAVs at their starting nodes. The change to the original formulation results in a significantly worse objective function

25

value of 18,904,435,773, with 60 units of supplies still delivered to demand nodes. UAV one's flight path is $1 \rightarrow 4 \rightarrow 1$ and expends 594,481 Wh of energy. UAV two's flight path is $2 \rightarrow 5 \rightarrow 1$ and expends 903,032 Wh of energy. UAV three's flight path is $3 \rightarrow 10 \rightarrow 9 \rightarrow 3$ and expends 761,393 Wh of energy. The flight path of the UAVs can be seen in Figure 3.2.
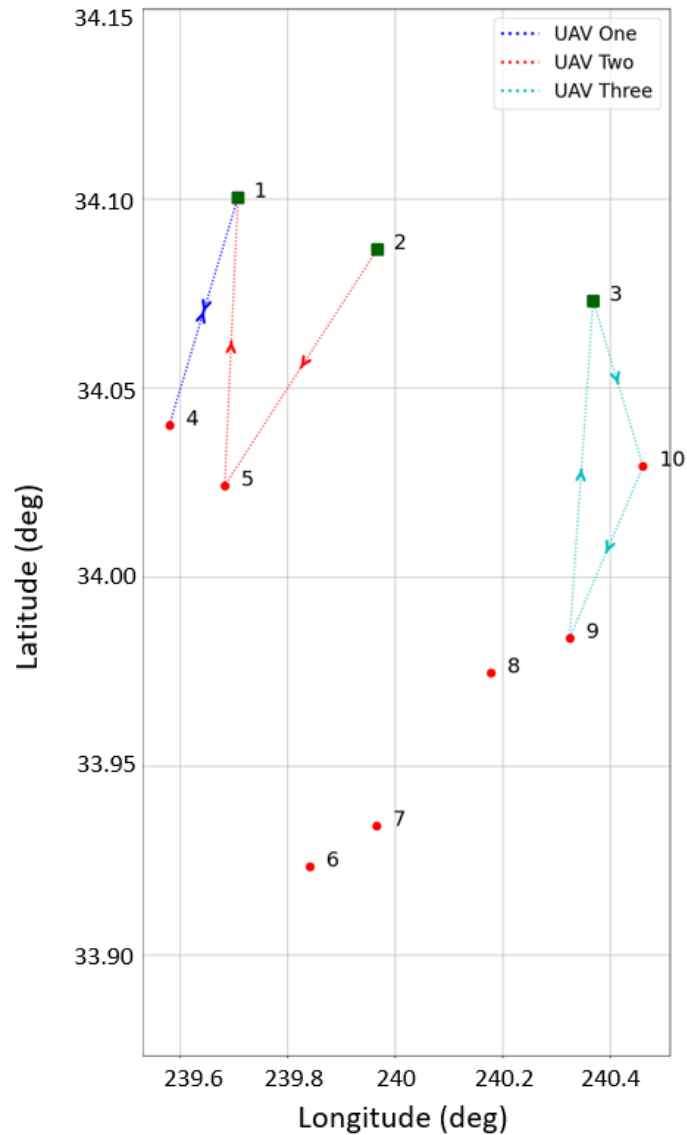
Figure 3.2. Flight path for all three UAVs.

Employing three UAVs compared to two UAVs results in a worse objective function while providing the same amount of support to demand nodes. This demonstrates the model's

ability to minimize UAV energy expenditure while maximizing the reward gained from providing support to the demand nodes.

3.10 Partial Delivery of Demand Node Requirements

In practice, some nodes may request multiple items that could be divided among multiple UAVs. We achieve partial delivery of demands by manipulating the cost matrix. If a node has more than one request, we create "dummy demand nodes" that represent the additional requests. The cost of flight to and from the "dummy demand nodes" are identical to the costs incurred by the original demand node. However, the cost to fly to and from the original demand node and the "dummy demand node" is set to zero. Figure 3.3 shows a network diagram displaying the cost matrix manipulation to achieve partial delivery.
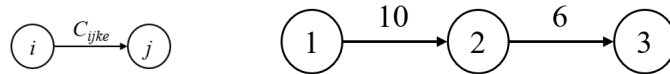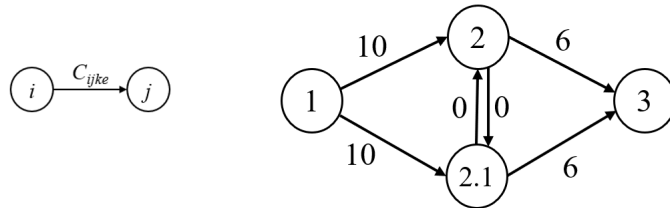
Figure 3.3. Cost matrix manipulation to achieve partial delivery.

We demonstrate the partial delivery capability using the scenario seen in Table 3.2 under the node network and wind profiles in Figure 2.6. Note that demand nodes four, five, nine and ten are each requesting two distinct packages in this scenario.

Table 3.2. Data for demand nodes and UAVs.

Demand Node	Demand Type and Amount
4	(1) 5 Urgent, (2) 5 Urgent
5	(1) 5 Urgent, (2) 5 Urgent
6	5 Urgent
7	5 Urgent
8	5 Urgent
9	(1) 5 Urgent, (2) 5 Urgent
10	(1) 5 Urgent, (2) 5 Urgent

UAV	Payload Capacity (lbs)	Energy (Wh)	Starting Depot
1	15	71,000	1
2	35	100,000,000	2
3	5	1,000,000	3

The total payload capacity of the three UAVs is 55 pounds and equal to the total demand seen across all demand nodes. To build intuition on partial deliveries, the energy and payload capacity on board UAVs one and three are reduced in order to limit their resupply capabilities. Meanwhile, UAV two's energy capacity is set at a large threshold of 100,000,000 Wh to allow it to resupply all remaining nodes not visited by UAVs one and three. The resulting flight paths of each UAV can be seen in Figure 3.4.
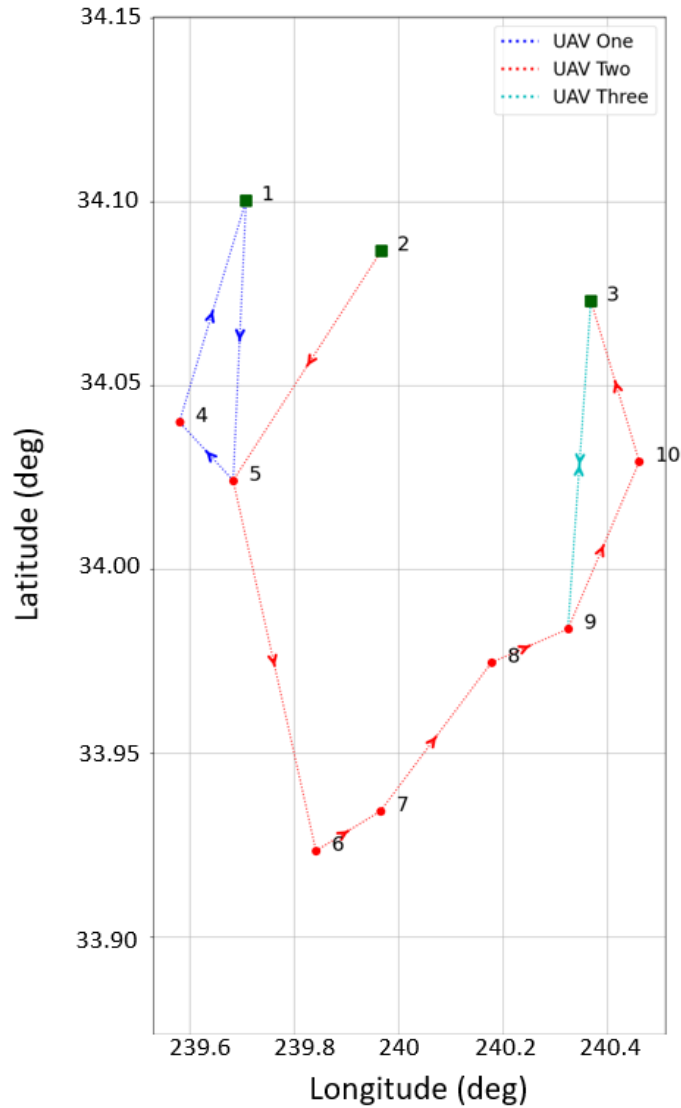
Figure 3.4. Flight path for all three UAVs in the partial delivery scenario.

UAV one's flight path is $1 \rightarrow 5 \rightarrow 4 \rightarrow 1$ and it supplies one of the two packages requested at demand node five. UAV two's flight path is $2 \rightarrow 5 \rightarrow 6 \rightarrow 7 \rightarrow 8 \rightarrow 9 \rightarrow 10 \rightarrow 3$ and it supplies one of the two packages at node five and node nine while fulfilling both demands at node ten. UAV three's flight path is $3 \rightarrow 9 \rightarrow 3$ and satisfies 50% of the requested supplies at node nine. As seen in this scenario, partial delivery provides flexibility for Marine logistics planners as it allows UAVs to collectively work together to fulfill supply demands across the network of nodes.

THIS PAGE INTENTIONALLY LEFT BLANK

CHAPTER 4:
Case Studies

4.1 Deterministic and Ensemble Model Comparison

To compare the difference in UAV routes between the ensemble weather model and a single deterministic weather forecast, we consider a scenario used by Haller (2021). Haller employs an operating environment that consists of two supply depots, two UAVs and nine demand nodes that are evenly distributed between the two supply depots. The network and general wind direction for this scenario can be seen in Figure 4.1.
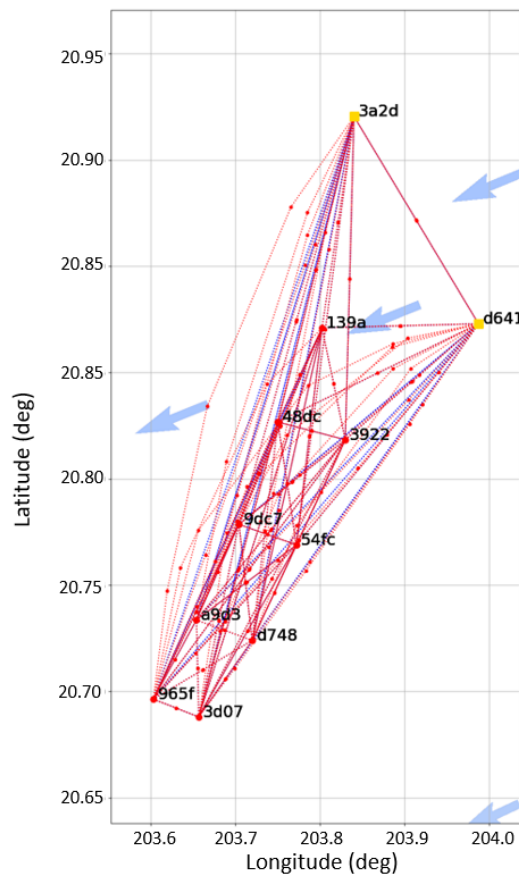
Figure 4.1. Network for comparison between deterministic and ensemble costs.

In this network, each demand node requires one package weighing three pounds. Demand nodes 3-8, which are the closest to the supply depots, are set to priority requests. Nodes 8-11 are farther away and are designated as urgent requests to incentivize the model to explore longer flights in return for larger rewards. Both prototype UAVs have batteries with 110,000 Wh of energy and a payload capacity of 15 pounds, which is sufficient to satisfy all demand (given sufficient energy capacity). Table 4.1 captures all input data for this scenario.

Table 4.1. Data for comparison between deterministic and ensemble costs.

Demand Node	Demand Type & Amount
3	3 priority
4	3 priority
5	3 priority
6	3 priority
7	3 priority
8	3 urgent
9	3 urgent
10	3 urgent
11	3 urgent

UAV	Payload Capacity (lbs)	Energy (Wh)	Starting Depot
1	15	1,100,000	1
2	15	1,100,000	2

The resulting flight paths can be seen in Figure 4.2. For the ensemble model, UAV One's flight path was $1 \rightarrow 3 \rightarrow 1$ and UAV Two's flight path was $2 \rightarrow 4 \rightarrow 6 \rightarrow 5 \rightarrow 1$. In the deterministic model, UAV One's flight path was $1 \rightarrow 3 \rightarrow 1$ and UAV flight path was $2 \rightarrow 4 \rightarrow 6 \rightarrow 8 \rightarrow 7 \rightarrow 5 \rightarrow 1$. The deterministic weather model allows the UAVs to visit six nodes while the ensemble weather model results in four nodes visited by the UAVs.
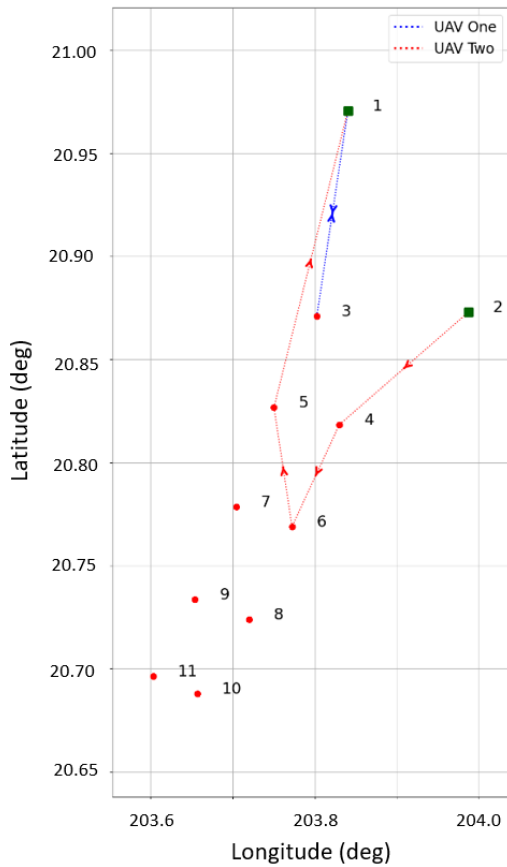
(a) Flight path for ensemble weather model.
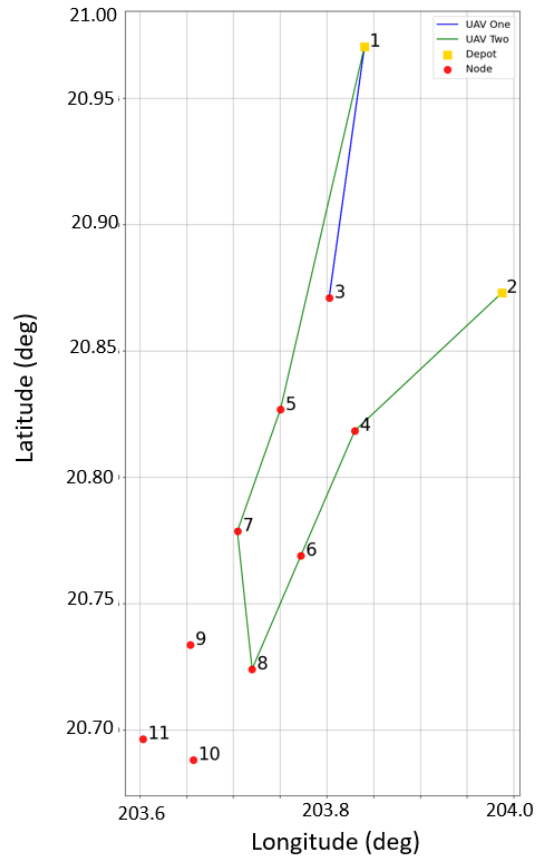
(b) Flight path for deterministic weather model.

Figure 4.2. Comparison of flight paths for ensemble and deterministic wind costs.

Table 4.2 displays the cost of flight for each ensemble member for UAV Two's flight path in the deterministic model. Five out of 10 ensemble members resulted in a cost of flight less than the UAV's energy capacity of 1,100,000 Wh of energy, which five resulted in energy expenditures exceeding this limit. In practice, this means that the route generated by the deterministic model has a significant likelihood of being infeasible due to the actual weather outcome being different than the expected outcome that was entered into the model.

Table 4.3 highlights the different statistics between the two models. The difference in objective function value for the ensemble model and the deterministic model was 49.2% and this was achieved with the deterministic model expending only 4.8% more energy than

Table 4.2. Energy cost for UAV two to fly the deterministic cost flight path for each ensemble member. The energy costs shaded in red exceed the UAV's energy capacity.

Ensemble	Cost (Wh)	Ensemble	Cost (Wh)
1	1,318,811.32	6	1,219,294.31
2	1,075,540.03	7	1,084,747.32
3	1,037,796.86	8	713,679.52
4	703,168.31	9	1,131,567.04
5	1,228,495.59	10	1,213,972.29

the ensemble weather model. The greater objective function value is the result of UAVs in the deterministic model being able to satisfy two more demands than the ensemble model, of which one was an urgent request. This comparison highlights the robustness of solution from the ensemble weather model. While the ensemble model produces a less positive output in regard to reward gained, it leads to a more conservative approach to UAV flight routing and a greater probability for mission accomplishment.

Table 4.3. Output from both models

	Ensemble	Deterministic
Objective Function Value	2,792,715,529.05	4,172,854,819.87
Total Nodes Visited	4	6
UAV1 Energy Expenditure	449,857.71	395,601.79
UAV2 Energy Expenditure	962,716.99	1,084,527.62
Total Energy Expenditure	1,412,574.70	1,480,129.41

4.2   Infantry Battalion Case Study

We now consider a hypothetical case study to display the utility of the ensemble weather model for EABO. For this case study, we consider an infantry battalion tasked with conducting sea denial operations in the Indo-Pacific Command area of operations. We assume the infantry battalion has direct support from a combat logistics battalion (CLB) and a combat logistics regiment (CLR) in close proximity to provide additional support.

To represent the UAVs being considered for employment by the USMC, we consider drone platforms under the USMC's Unmanned Logistics Systems - Air (ULS-A) program. The ULS-A program divides the platforms into small, medium, and large categories, where payload capacity and range increase with larger platforms. As expected, platforms with greater logistics capabilities are to be fielded by logistics units while the ULS-A small platform are tailored towards infantry battalions. The characteristics and intended organization for each platform are taken from Borrelli (2019) and shown in Table 4.4. CLR, Marine Logistics Group (MLG), and CLB are current logistics units within the USMC. To understand the hierarchy of these units, a MLG provides direct support to the Ground Combat Element (GCE) and consists of two CLRs which are made up of three CLBs.

Table 4.4. ULS-A platform characteristics.

ULS-A System	Range (km)	Payload Capacity (lbs)	Estimated Platforms per Organization	Demand Unit Size
Large	408	20,000	6 per CLR	Company
Medium	70	5,000	30 per MLG; 10 Per CLB	Platoon
Small	20	55	10 per infantry battalion	Squad

4.2.1 Scenario

An infantry battalion consists of three rifle companies, one weapons company and a headquarters and services (H&S) company. Each rifle company has three rifle platoons and one weapons platoon, and each weapons company consists of anti-armor teams, snipers, and a 81 mm mortar platoon. The H&S company consists of support personnel in areas such as logistics, communications, intelligence, and administration.

Figure 4.3 displays the force layout of an infantry battalion conducting sea denial operations. CLR is trailing the main body of the battalion and is situated on the most eastern body of land at depot one. The position of the CLR allows the infantry battalion to request support from the CLR via the CLB. CLB is centrally located relative to the forward operating units at depot two and considered to be in direct support of the infantry battalion. Squad-sized elements are spread across the islands while two companies are staged on the most western and southern islands in the area of operations. We assume weapons company to be attached

to the three line companies and personnel in the H&S company are staged at depots three and four.
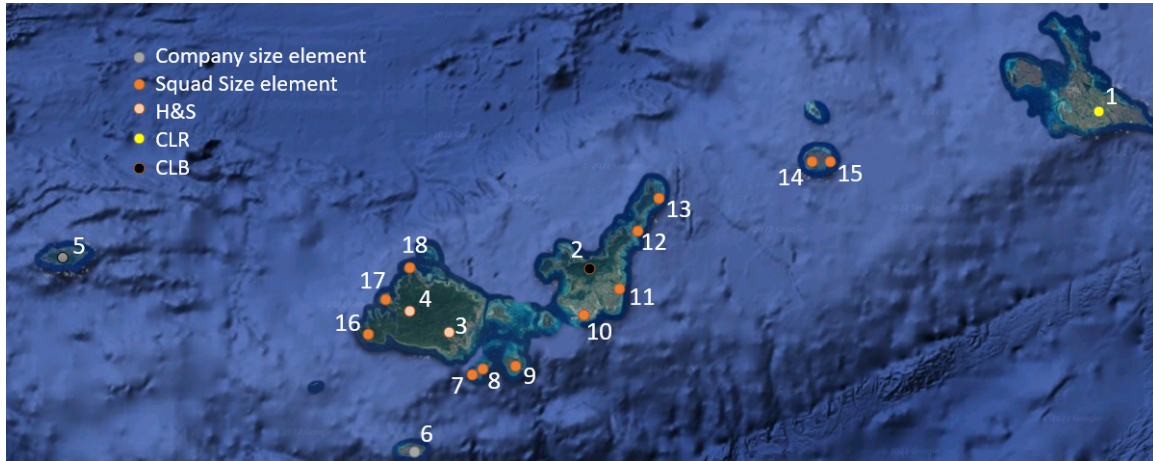

Figure 4.3. Force layout for scenario resupplying infantry battalion.

We determine energy capacity for the ULS-A large platform by summing energy required to travel flight segments that result in a total distance of 408 km, since this is the published range of the ULS-A large platform. In this scenario, the sequential distance between nodes one, six, five, sixteen and one meets the requirement of 408 km and has an average energy consumption of a 10,929,756 Wh across all ten ensemble members. The energy for the ULS-A medium and small platforms are set relative to the large platform and determined to be 1,593,919 Wh and 546,488 Wh respectively. One ULS-A large, five ULS-A medium, and six ULS-A small platforms are dedicated for this scenario. payload capacity across all UAVs is set to 45,330 lbs and the infantry battalion seeks a total resupply of 27,013 lbs across 41 demand nodes. Priority levels for demands at nodes five and six are set at an urgent level while the priority levels for all other demand nodes are randomized across the three priority levels. The starting nodes, energy, and capacity of the UAVs along with the demands at each node are show on Table 4.5. To identify which demand is satisfied for multi-demand nodes, additional demands are distinguished by float variables. For example, node seven contains three demands that can be partially fulfilled by the UAVs. The first demand is associated with node 7 while the subsequent demands are associated with nodes 7.1 and 7.2.

Table 4.5. Demand node and UAV characteristics for infantry battalion scenario (U = Urgent, P = Priority, and R = Routine).

Demand Node	Demand Type and Amount	Total Demand
5	(1) 1,500 U, (2) 1,500 U, (3) 1,000 U, (4) 1,000 U (5) 1,900 U, (6)1,670 U	8,570
6	(1) 1,750 U, (2) 3,500 U, (3) 3,000 U, (4) 4,080 U	12,330
7	(1) 2,500 U, (2) 500 P, (3) 40 R	3,040
8	(1) 500 P, (2) 250 R, (3) 10 U, (4) 5 U	765
9	(1) 750 U, (2) 100 P, (3) 125 R	975
10	(1) 55 R, (2) 30 U, (3) 30 U	115
11	(1) 400 U, (2) 300 R, (3) 10 U	710
12	(1) 30 P, (2) 5 U	35
13	(1) 40 U, (2) 20 R	60
14	(1) 55 U	55
15	(1) 10 U, (2) 20 P	30
16	(1) 60 U, (2) 35 P, (3) 10 P	105
17	(1) 70 P, (2) 30 U	100
18	(1) 90 R, (2) 10 U, (3) 23 R	123

UAV	Payload Capacity (lbs)	Energy (Wh)	Starting Depot
1	20,000	10,929,756	1
2	5,000	1,593,919	2
3	5,000	1,593,919	2
4	5,000	1,593,919	2
5	5,000	1,593,919	2
6	5,000	1,593,919	2
7	55	546,488	3
8	55	546,488	3
9	55	546,488	3
10	55	546,488	4
11	55	546,488	4
12	55	546,488	4

The resulting optimization problem consists of 24,295 variables and 2,394 linear constraints. We solve the model using the CPLEX (version 22.1.0.0) solver within the Pyomo (version 6.1.2) software package. The solver requires 1,507.11 seconds to solve the problem to a 10% optimality gap. The flight paths for the UAVs can be seen in Figure 4.4, and Table 4.6 outlines the statistics of the flight segments taken by the UAVs.
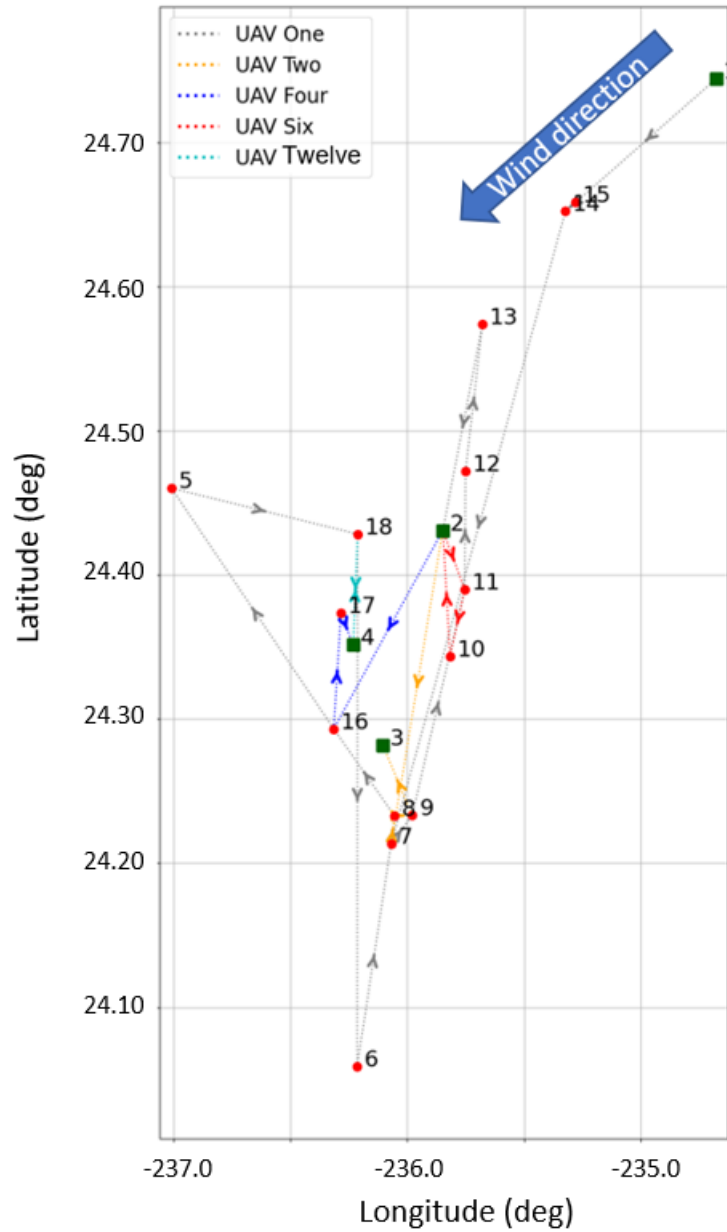
Figure 4.4. UAVs flight paths for infantry battalion scenario.

Analysis

Five of the 12 UAVs are utilized to fulfill 39 out of 41 demands for a total of 24,003 pounds of supplies delivered to the demand nodes. The objective function value is 141,462,261,396 which is 10,177,375,924 less than the best possible solution of 151,639,637,320 determined

Table 4.6. Flight statistics for infantry battalion scenario.

UAV	Flight Path (Nodes)	Total Resupply (lbs)	Percentage of Capacity Resupplied	Energy Expenditure (Wh)	Percentage of Energy Expended
One	1 → 15.1 → 14 → 7.2 →8 → 8.2 → 8.1 →16 →5.1 → 5 → 5.2 → 5.5 → 5.4 →5.3 → 18 → 6.1 →6 → 6.3 → 7.1 →9.1 →11.1 → 11.2 → 12.1 → 12 → 13.1 → 13 → 2	19,930	99.65%	10,406,848	95.20%
Two	2 → 7 → 8.3 → 9.2 → 9 → 3	3,380	67.60%	1,219,109	76.5%
Four	2 → 16.2 → 16.1 → 17.1 → 17 → 4	145	2.90%	1,389,295	87.20%
Six	2 → 11 → 10.1 → 10 → 10.2 → 2	515	10.30%	617,387	38.70%
Twelve	4 → 18.2 → 18.1 → 4	33	60%	373,248	68.30%

by the solver via linear relaxation. UAV One, the ULS-A large platform assigned to the CLR, conducts a majority of the resupplies as it fulfills 25 demands at 12 different nodes. UAV One's flight consumes 95.20% of its energy and utilizes 99.65% of its payload capacity.

Due to the optimality gap of 10%, some suboptimal UAV routes are selected by the solver. For example, UAV One visits node 7.2 on the third segment of its flight only to return to node 7.1 on the 18th segment of its flight. UAV One can save energy by resupplying node 7.1 while fulfilling the demand at node 7.2. Another inefficient route is seen when UAV 12 visits demand nodes 18.2 and 18.1 to fulfill a total demand of 33 lbs. UAV One visits node 18 on the 14th segment of its flight and holds enough supplies to fulfill the demands at nodes 18.1 and 18.2. By allowing UAV One to conduct the resupply for 18.1 and 18.2, the model can conserve 373,248 Wh of energy.

Considerations

In practice, users must consider the return depot for larger UAV platforms. Larger and more technologically advanced platforms likely require a certain level of specialized equipment and capabilities that is not required by smaller platforms. In this scenario, UAV One (large size) returns to supply depot two which is operated by the CLB, and UAV Two (medium size) returns to a depot operated by the infantry battalion. Since these depots are owned by units without large and medium ULS-A UAVs, it is unlikely the personnel at these depots will be able to refit and recharge these UAVs for follow on missions.

The concept of employment seen from the solver contradicts the USMC concept of logistics. USMC concept of logistics seeks to provide support with organic and attached assets prior to requesting assistance from higher headquarters. In this scenario, only 36% of the organic and attached assets are utilized to fulfill 34% of the 41 demands. UAV One, an asset above the infantry battalion, resupplies 60% of the total demands. Methods to increase organic support are explored in the next section.

4.2.2   Increase Organic Support

To gain further insight into methods to increase organic support, we consider a scenario where the location of demand nodes and requested demands stay consistent with the previous scenarios. However, the new scenario increases the total number of depots for H&S from two to four and the depots placed closer to the demand nodes. The layout of the forces is show in Figure 4.5.
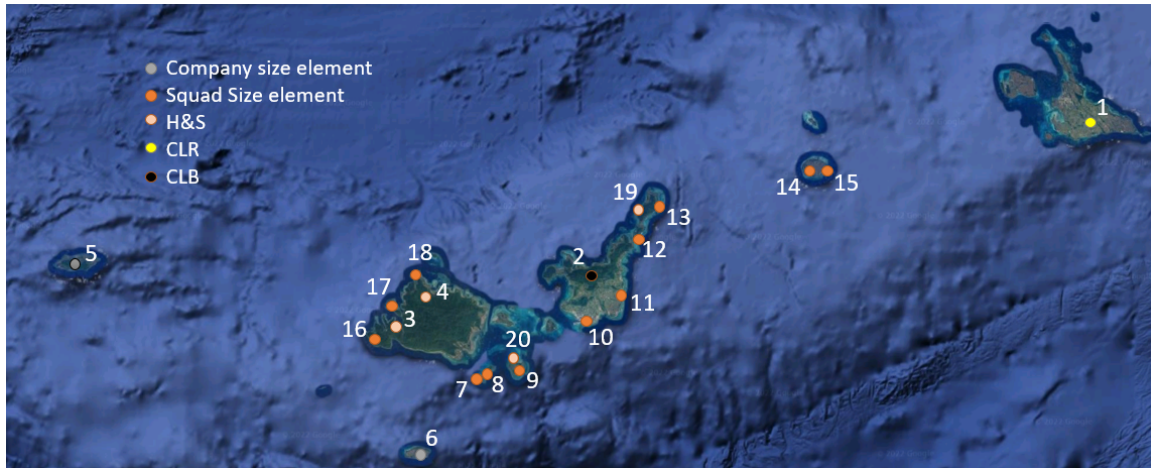
Figure 4.5. Force layout to increase organic support.

The H&S depots are strategically placed within close proximity of demand nodes that are requesting packages below the 55 lb payload capacity seen in small UAVs. Within the 41 requested demands in the network, 19 of the demands can be supplied by the small UAVs. The 19 demands reside within nodes 7 through 18 and have a total demand of 468 lbs. However, nodes 14 and 15 are 43 Km from the nearest H&S depot and are out of range of small UAVs. The one-way distance from the H&S depot nodes to the neighboring nodes are shown in Table 4.7.

Table 4.7. One-way distances from HS depots to neighboring demand nodes

Depot Node	Distances to Demand Nodes
3	(17) 5 Km, (18) 5.8 Km
4	(16) 5.7 Km, (17) 6.4 Km
19	(11) 12.15 Km, (12) 3.9 Km, (13) 9.3 Km
20	(7) 7.8 Km, (8) 6.22 Km, (9) 1.7 Km, (10) 19.6 Km

The number of small UAVs are increased from six to ten to resemble the number of small UAVs that are expected to be fielded by infantry battalions; this implements the increased organic support. The scenario does not involve any medium- or large-sized UAVs. The starting depots for the UAVs are shown in Table 4.8.

Table 4.8. Force layout to increase organic support.

UAV	Capacity (lbs)	Energy (Wh)	Starting Depot
1	55	546,488	3
2	55	546,488	3
3	55	546,488	3
4	55	546,488	4
5	55	546,488	4
6	55	546,488	4
7	55	546,488	19
8	55	546,488	19
9	55	546,488	20
10	55	546,488	20

This scenario employs one UAV to satisfy two demands at node 18 for a total of 33 lbs. Rest of the UAVs are not assigned any resupply missions as the UAVs do not have enough energy to conduct resupply missions and return back to a supply depot.

With this insight, the energy capacity of the UAVs are increased to 1,070,203 Wh, a value that is between the energy capacity of the small and medium UAV. The increase in energy capacity results in the employment of five UAVs to satisfy seven of the 19 demands that are below the 55 lbs threshold. The UAVs collectively deliver 39 % of the 468 lbs present within the 19 demands. The flight statistics can be seen in Table 4.9.

Table 4.9. UAV flight statistics for increase in energy capacity for small UAVs.

UAV	Flight Path (Nodes)	Total Resupply (lbs)	Percentage of Capacity Resupplied	Energy Expenditure (Wh)	Percentage of Energy Expended
3	3→18.1→18.2→3	33	66.70%	137,900	12.89%
4	4→10→4	55	100%	1,060,862	99.13%
5	4→10.1→4	30	54.54%	1,060,862	99.13%
6	4→10.2→4	30	54.54%	1,060,862	99.13%
10	20→12→12.1→2	35	63.63%	1,068,662	99.86%

The final iteration of the scenario increases the energy capacity of the small UAVs to 1,593,919 which is the same energy capacity of a medium UAV. This results in 13 of 19 demands being fulfilled to satisfy 69% of the total lbs requested by the demand nodes. The increase in energy capacity allows more UAVs to be employed by the model and 80% of the small UAVs depart their starting depots for demand nodes.

Table 4.10. UAV flight statistics for small UAVs with energy capacity seen in medium UAVs.

UAV	Flight Path (Nodes)	Total Resupply (lbs)	Percentage of Capacity Resupplied	Energy Expenditure (Wh)	Percentage of Energy Expended
1	3→18.1→18.2→3	33	60.00%	137,900	8.65%
2	3→12.1→13→2	45	81.82%	1,319,803	82.80%
3	3→13.1→12→2	50	90.91%	1,456,486	91.38%
4	4→10.2→11.2→2	40	72.73%	1,220,689	76.58%
5	4→10→4	55	100.00%	1,060,862	66.56%
6	4→10.1→4	30	54.55%	1,060,862	66.56%
7	19→8.2→8.3→3	15	27.27%	1,297,397	81.40%
9	20→14→2	55	100.00%	1,391,078	87.27%

Analysis

To maximize organic support prior to requesting support from higher command, this instance requires the solver to return an initial output of nodes serviced by organic assets. The logistics cell must then identify the unfilled demands and request support from logistics units with greater capabilities. To automate the process of increasing organic support, the model can be modified to prioritize the employment of organic UAVs prior to developing routes for UAVs at higher levels of command.

While the situation of the operating environment will determine the number of depots and their proximity to stand-in forces, the closer the depots are to the stand-in forces and greater energy capacities on small UAVs lead to increased utilization of organic assets. From experience in the fleet, four supply depots (or combat service support area) are most likely the maximum number of depots that are able to be manned by an infantry battalion. The three iterations showed the number of demand nodes satisfied increasing from one, seven to 13, as the energy capacity increased from 546,488 Wh, 1,070,203 Wh and 1,593,919 Wh. With this insight, we recommend the ULS-A program to optimize the battery capacity of the small UAVs in accordance with the stand-off distance (distance from depot to stand-in forces) of the supply depots and the expected number of supply depots required to be manned by infantry battalion H&S companies.

THIS PAGE INTENTIONALLY LEFT BLANK

CHAPTER 5:
Conclusion and Future Work

5.1 Conclusion

This thesis expands on the work conducted by Jatho (2020) and Haller (2021) to include ensemble wind costs and partial deliveries. Our objective function includes multiple terms designed to maximize satisfaction of prioritized requests with a tiebreaker to minimize energy consumption. This ensures the selected UAV routes are holistic in nature and account for both rewards and energy costs. The implementation of the ensemble cost matrix ensures the solutions are more robust compared to solutions provided by Haller (2021), leading to higher probability of mission success. Partial deliveries provide logistic planners with greater flexibility by allowing UAVs to work in a synchronized matter. Overall, the work conducted in this thesis improves energy based routing of UAVs to support the Marines operating in hostile locations at various EABs.

5.2 Future Work

The work described in this thesis can be extended in many interesting and important ways.

5.2.1 Integration With Warfighting functions

Our model can be improved by integrating information from other warfighting functions. In combat operations, command and control centers maintain situational awareness through a common tactical picture (CTP). They are up to date on information such as fire support missions, positions of enemy and friendly troops, information on troops in contact, status of supplies of forward troops, no-fly zones, requests from friendly forces, etc. Integrating data from the CTP will allow the model to optimize UAV routes in a harmonious manner with activity occurring in the battlefield.

5.2.2 Delivery Window

Stand-in forces may not have the ability to communicate with higher headquarters, as frequently seen in previous conflicts due to signature management and degraded communications. Delivery windows provide the ability for stand-in forces to forecast their supplies and proactively send logistics requests for future delivery windows. This concept will remove the limitation of logistics requests being tied to communication windows.

5.2.3 Type and Compatibility of Supplies

Currently the packages requested by the demand nodes are not distinguished by item type. This leads to an assumption that all supply depots are infinitely stocked with all requested packages. Classifying the demands by type and establishing a stock level at each supply depot will ensure UAV k at supply depot i will only visits demand node j if it has the demanded item type.

Once supplies are classified by type, compatibility of supplies need to be explored as well. Certain supplies are not compatible and may not be transported together in the same compartment. These issues are most prevalent with ammunition and hazardous material. Establishing compatibility of supplies within the model will increase the flexibility of the model for the USMC logistician.

5.2.4 Alternate Supply Depots and Multiple Trips

In the current model, UAVs start with the supplies in their starting depot and do not have the option to visit neighboring supply depots to fill their payloads. Once supplies are classified by type at the demand nodes and the supply depots, future models should be expanded to allow UAVs to visit alternative supply depots to pick up the specific supplies requested by the demand nodes. This requires a generalization of the model to include multiple depot visits within the planning horizon, and it can also be extended to include battery recharge or swaps.

5.2.5 Develop constraints for UAV Return Depot

The infantry battalion scenario resulted in the large UAV returning to depots that were home depots for small UAVs. Larger UAVs most likely require specialized tools and personnel

with greater maintenance capabilities to refit and recharge the UAVs for follow on missions. Follow on work should develop constraints that limit the UAVs to return to depots that possess the required capabilities to support the technical specifications of the platform.

5.2.6   Decrease Solver Time

Compared to the deterministic model, the ensemble members and the ability to conduct partial delivery in the ensemble weather model increases the complexity of the problem. The ensemble weather members in the cost matrix increase the number of constraints while partial delivery increases the number of nodes within each of set of costs per ensemble member. Table 5.1 shows the size of the cost matrix for various number of ensemble members and partial delivery. The first row in Table 5.1 resembles a deterministic cost matrix in a 10 node network. As the number of ensemble members and partial delivery increase, the size of the cost matrix increases as well.

Table 5.1. Size of the cost matrix for various number of ensemble members and partial deliveries.

Number of Nodes	Number of Ensemble Members	Number of Partial Deliveries	Size of Cost Matrix
10	0	0	100
10	2	1	242
10	3	2	432
10	4	3	676
10	5	4	980
10	6	5	1,350
10	7	6	1,792
10	8	7	2,312
10	9	8	2,916
10	10	9	3,610

At the second OR layer, the most complex scenario in Haller (2021) thesis consisted of 1,536

decision variables and 357 constraints resulting in a solver time of 229 seconds. The entry level complexity of the battalion-level scenario in this thesis consisted of 24,295 decision variables and 2,394 constraints and when solved to a 10% optimality gap, resulted in a solver time of 25 minutes. Higher complexity scenarios tested to increase organic support needed a minimum of one week on the computers in the Naval Postgraduate School's optimization lab to achieve a 10% optimality gap. Thus, we recommend that future work explore possible reformulations or heuristics in order to shorten the solver run time.

Another recommended solution to decrease solver time is to eliminate the arcs between nodes i and j that have costs greater than the energy capacities of the UAVs. By eliminating these arcs, the solver has fewer x_{ijk} decision variables to consider resulting in a faster time to solve the MDVRP.

5.2.7 Third Layer

The first battalion-level scenario displayed the inefficiencies in UAV routing when solved to a 10% optimality gap. A third layer can be implemented to correct the inefficient routes. By resolving the model with each UAV constrained to satisfy the demands it was selected to support in the second layer, the problem becomes much smaller and an optimal routing can be produced by the solver more quickly.

5.3 Final Thoughts

As we prepare for combat against near-peer adversaries, employment of technologically advanced capabilities must be considered for all warfighting functions. In the field of logistics, UAVs provide a low-risk but high-payoff platform required to support distributed stand-in forces conducting EABO. Logistics UAVs backed by robust routing models will ensure Marines are sustained and postured for combat operations. As Marine logisticians are fielded the capability of autonomous UAVs, the models in this thesis will assist in planning and execution of combat operations.

List of References

Berger (2019) Commandant's planning guidance. hhttps://www.marines.mil/News/News-Display/Article/2707972/2019-commandants-planning-guidance/.

Borrelli (2019) USMC Unmanned Logistics Systems – Air ULS-A overview for Office of Naval Research.

Cheng C, Adulyasak Y, Rousseau LM (2018) *Formulations and exact algorithms for drone routing problem*. Centre Interuniversitaire de Recherche sur les Réseaux d'Entreprise, la Logistique et le Transport (CIRRELT), Montreal, Canada .

Craparo E, Karatas M, Singham D (2017) A robust optimization approach to hybrid microgrid operation using ensemble weather forecasts. *Journal of Applied Energy* 201(13):135–147.

Dobrokhodov V, Jones KD, Walton C, Kaminer II (2020) Energy-optimal trajectory planning of hybrid ultra-long endurance UAV in time-varying energy fields. *AIAA Scitech 2020 Forum* (American Institute of Aeronautics and Astronautics), https://doi.org/10.2514/6.2020-2299.

Dorling K, Heinrichs J, Messier G, Magierowski S (2018) Vehicle routing problems for drone delivery. *IEEE Transactions on Systems, Man, and Cybernetics: Systems* 47(1):70–85, https://doi.org/10.1109/TSMC.2016.2582745.

Franco A, Rivas D, Valenzuela A (2017) Optimal aircraft path planning considering wind uncertainty. volume 7, 1–11 (European Conference for Aeronautics and Space Sciences).

Haller J (2021) Expanding optimization of energy effective UAV routing in support of Marine Corps Expeditionary Advanced Base Operations with multiple supply depots. Thesis, Department of Operations Research, Naval Postgraduate School.

Jaillet P, Lu X (2011) Online traveling salesman problems with service flexibility. *Networks* 58(2):137–146.

Jatho A (2020) Optimizing energy efficient UAV routing in support of Marine Corps Expeditionary Advanced Base Operations. Thesis, Department of Operations Research, Naval Postgraduate School.

Kaempfer Y, Wolf L (2019) Learning the multiple traveling salesmen problem with permutation invariant pooling networks. *arXiv:1803.09621 [cs, stat]* https://arxiv.org/abs/1803.09621.

Kara I, Bektas T (2006) Integer linear programming formulations of multiple salesman problems and its variations. *European Journal of Operational Research* 174(3):1449–1458.

Leutbecher M, Palmer T (2007) A review of single and population-based metaheuristic algorithms solving multi depot vehicle routing problem. *Journal of Computational Physics* 227(25):3515–3539.

Miller CE, Tucker AW, Zemlin RA (1960) Integer programming formulation of traveling salesman problems. *J. ACM* 7(4):326–329, https://doi.org/10.1145/321043.321046.

Samsuddin S, Othman MS, Yusuf LM (2018) Ensemble forecasting. *International Journal of Software Engineering and Computer Systems (Pahang)* 4(2):80–93.

United States Marine Corps (2018) Expeditionary Advanced Base Operations Handbook. https://mca-marines.org/wp-content/uploads/Expeditionary-Advanced-Base-Operations-EABO-handbook-1.1.pdf.

Initial Distribution List

1. Defense Technical Information Center
   Ft. Belvoir, Virginia

2. Dudley Knox Library
   Naval Postgraduate School
   Monterey, California